Research Article | Vol. 25, No. 4 | 20 Feb 2017 | OPTICS EXPRESS 2998

Optics EXPRESS

Real-time imaging of methane gas leaks using a single-pixel camera

GRAHAM M. GIBSON,[1,*] BAOQING SUN,[1] MATTHEW P. EDGAR,[1] DAVID B. PHILLIPS,[1] NILS HEMPLER,[2] GARETH T. MAKER,[2] GRAEME P. A. MALCOLM,[2] AND MILES J. PADGETT [1]

[1]*SUPA, School of Physics and Astronomy, University of Glasgow, Glasgow, G12 8QQ, UK*
[2]*M Squared Lasers Ltd, 1 Kelvin Campus, West of Scotland Science Park, Maryhill Road, Glasgow, G20 0SP, UK*
[*]*Graham.Gibson@glasgow.ac.uk*
http://www.gla.ac.uk/schools/physics/research/groups/optics/

Abstract: We demonstrate a camera which can image methane gas at video rates, using only a single-pixel detector and structured illumination. The light source is an infrared laser diode operating at 1.651μm tuned to an absorption line of methane gas. The light is structured using an addressable micromirror array to pattern the laser output with a sequence of Hadamard masks. The resulting backscattered light is recorded using a single-pixel InGaAs detector which provides a measure of the correlation between the projected patterns and the gas distribution in the scene. Knowledge of this correlation and the patterns allows an image to be reconstructed of the gas in the scene. For the application of locating gas leaks the frame rate of the camera is of primary importance, which in this case is inversely proportional to the square of the linear resolution. Here we demonstrate gas imaging at ~25 fps while using 256 mask patterns (corresponding to an image resolution of 16x16). To aid the task of locating the source of the gas emission, we overlay an upsampled and smoothed image of the low-resolution gas image onto a high-resolution color image of the scene, recorded using a standard CMOS camera. We demonstrate for an illumination of only 5mW across the field-of-view imaging of a methane gas leak of ~0.2 litres/minute from a distance of ~1 metre.

OCIS codes: (110.1758) Computational imaging; (110.3080) Infrared imaging; (040.1490) Cameras; (100.3010) Image reconstruction techniques.

References and links

1. E. Naranjo, S. Baliga, and P. Bernascolle, "IR gas imaging in an industrial setting," (SPIE, 2010), vol. 7661 of *Thermosense XXXII*.
2. M. Gålfalk, G. Olofsson, P. Crill, and D. Bastviken, "Making methane visible," Nature Clim. Change **6**, 426–430 (2016).
3. C. F. Simpson and T. A. Gough, "Direct quantitative analysis using flame ionisation detection. the construction and performance of the FIDOH detector," J. Chromatogr. Sci. **19**, 275–282 (1981).
4. B. R. Cosofret, W. J. Marinelli, T. Ustun, C. M. Gittins, M. T. Boies, M. F. Hinds, D. C. Rossi, R. Coxe, S. Chang, B. D. Green, and T. Nakamura, "Passive infrared imaging sensor for standoff detection of methane leaks," (SPIE, 2004), vol. 5584 of *Chemical and Biological Standoff Detection II*, pp. 93–99.
5. T. J. Kulp, P. Powers, R. Kennedy, and U.-B. Goers, "Development of a pulsed backscatter-absorption gas-imaging system and its application to the visualization of natural gas leaks," Appl. Opt. **37**, 3912–3922 (1998).
6. J. Sandsten, P. Weibring, H. Edner, and S. Svanberg, "Real-time gas-correlation imaging employing thermal background radiation," Opt. Express **6**, 92–103 (2000).
7. G. Gibson, B. v. Well, J. Hodgkinson, R. Pride, R. Strzoda, S. Murray, S. Bishton, and M. Padgett, "Imaging of methane gas using a scanning, open-path laser system," New J. Phys. **8**, S1367 (2006).
8. D. Stothard, M. Dunn, and C. Rae, "Hyperspectral imaging of gases with a continuous-wave pump-enhanced optical parametric oscillator," Opt. Express **12**, 947–955 (2004).
9. T. Iseki, H. Tai, and K. Kimura, "A portable remote methane sensor using a tunable diode laser," Meas. Sci. Technol. **11**, 594–602 (2000).

#279984 https://doi.org/10.1364/OE.25.002998
Journal © 2017 Received 3 Nov 2016; revised 6 Jan 2017; accepted 6 Jan 2017; published 6 Feb 2017

Optics EXPRESS

10. B. v. Well, S. Murray, J. Hodgkinson, R. Pride, R. Strzoda, G. Gibson, and M. Padgett, "An open-path, hand-held laser system for the detection of methane gas," J. Opt. A: Pure Appl. Opt. **7**, S420–S424 (2005).
11. T. J. Kulp, P. E. Powers, and R. Kennedy, "Remote imaging of controlled gas releases using active and passive infrared imaging systems," (SPIE, 1997), vol. 3061 of *Infrared Technology and Applications XXIII*, pp. 269–278.
12. M. F. Duarte, M. A. Davenport, D. Takhar, J. N. Laska, T. Sun, K. F. Kelly, and R. G. Baraniuk, "Single-pixel imaging via compressive sampling," IEEE Signal Process. Mag. **25**, 83–91 (2008).
13. W. K. Pratt, J. Kane, and H. C. Andrews, "Hadamard transform image coding," Proc. IEEE **57**, 58–68 (1969).
14. R. I. Stantchev, B. Sun, S. M. Hornett, P. A. Hobson, G. M. Gibson, M. J. Padgett, and E. Hendry, "Noninvasive, near-field terahertz imaging of hidden objects using a single-pixel detector," Sci. Adv. **2**, e1600190 (2016).
15. N. Radwell, K. J. Mitchell, G. M. Gibson, M. P. Edgar, R. Bowman, and M. J. Padgett, "Single-pixel infrared and visible microscope," Optica **1**, 285–289 (2014).
16. J. B. Sampsell, "Digital micromirror device and its application to projection displays," J. Vac. Sci. Technol. B **12**, 3242–3246 (1994).
17. G. McConnell, S. Poland, and J. M. Girkin, "Fast wavelength multiplexing of a white-light supercontinuum using a digital micromirror device for improved three-dimensional fluorescence microscopy," Rev. Sci. Instrum. **77**, 013702 (2006).
18. M. P. Edgar, G. M. Gibson, R. W. Bowman, B. Sun, N. Radwell, K. J. Mitchell, S. S. Welsh, and M. J. Padgett, "Simultaneous real-time visible and infrared video with single-pixel detectors," Sci. Rep. **5**, 10669 (2015).
19. E. S. Voropai, I. M. Gulis, A. G. Kupreev, K. N. Kaplevskii, A. G. Kostyukevich, A. E. Radko, and K. A. Shevchenko, "Multi-object spectrometer with micromirror array," J. Appl. Spectrosc. **77**, 285–292 (2010).
20. R. D. Meyer, K. J. Kearney, Z. Ninkov, C. T. Cotton, P. Hammond, and B. D. Statt, "RITMOS: a micromirror-based multi-object spectrometer," Proc. SPIE **5492**, 200–219 (2004).
21. B. Sun, M. P. Edgar, R. Bowman, L. E. Vittert, S. Welsh, A. Bowman, and M. J. Padgett, "Differential computational ghost imaging," in "Imaging and Applied Optics," (OSA, Arlington, Virginia, 2013), no. CTu1C.4 in Computational Optical Sensing and Imaging.
22. L. Rothman, I. Gordon, Y. Babikov, A. Barbe, D. C. Benner, P. Bernath, M. Birk, L. Bizzocchi, V. Boudon, L. Brown, A. Campargue, K. Chance, E. Cohen, L. Coudert, V. Devi, B. Drouin, A. Fayt, J.-M. Flaud, R. Gamache, J. Harrison, J.-M. Hartmann, C. Hill, J. Hodges, D. Jacquemart, A. Jolly, J. Lamouroux, R. L. Roy, G.Li, D. Long, O. Lyulin, C. Mackie, S. Massie, S. Mikhailenko, H. Müller, O. Naumenko, A. Nikitin, J. Orphal, V. Perevalov, A. Perrin, E. Polovtseva, C. Richard, M. Smith, E. Starikova, K. Sung, S. Tashkun, J. Tennyson, G. Toon, V. Tyuterev, and G. Wagner, "The HITRAN2012 molecular spectroscopic database," J. Quant. Spectrosc. Radiat. Transfer **130**, 4–50 (2013).
23. D. B. Phillips, M.-J. Sun, J. M. Taylor, M. P. Edgar, S. M. Barnett, G. M. Gibson, and M. J. Padgett, "Adaptive foveated single-pixel imaging with dynamic super-sampling," arXiv preprint arXiv:1607.08236 (2016).
24. D. Takhar, J. N. Laska, M. B. Wakin, M. F. Duarte, D. B. S. Sarvotham, K. F. Kelly, and R. G. Baraniuk, "A new compressive imaging camera architecture using optical-domain compression," (SPIE, 2006), vol. 6065 of *Proc. of SPIE-IS&T Electronic Imaging*, pp. 606509.
25. M. Aβmann and M. Bayer, "Compressive adaptive computational ghost imaging," Sci. Rep. **3**, 1545 (2013).
26. M.-J. Sun, M. P. Edgar, D. B. Phillips, G. M.Gibson, and M. J. Padgett, "Improving the signal-to-noise ratio of single-pixel imaging using digital microscanning," Opt. Express **24**, 10476–10485 (2016).
27. N. K. Dhar, R. Dat, and A. K. Sood, *Optoelectronics - Advanced Materials and Devices* (InTech, 2013) Chap. 7, pp. 149–190.
28. K. W. Allen, F. Abolmaali, J. M. Duran, G. Ariyawansa, N. I. Limberopoulos, A. M. Urbas, and V. N. Astratov, "Increasing sensitivity and angle-of-view of mid-wave infrared detectors by integration with dielectric microspheres," Appl. Phys. Lett. **108**, 241108 (2016).

1. Introduction

The ability to image invisible gases has applications in industrial and environmental monitoring settings [1, 2], but is technologically challenging to embed in a low-cost device. For example, imaging methane gas has applications amongst gas utility companies for routine pipeline monitoring and storage facility inspection. Video rate gas imaging conveys the direction of dispersal and hence the location of a leak source, helping users to improve their efficiency of response to hazardous events. Conventional approaches to detecting methane gas leaks have mainly been based upon flame ionization detectors (FIDs) [3] but such technology measures concentration at only a single point, making locating the source of the leak a difficult and slow process.

One approach to gas imaging is to use a focal plane array (FPA) to image the methane directly. These array based systems can be passive, based on the absorption of ambient background radiation [4] or active, based on the optical absorption of laser light used as an illumination source [5]. Passive systems for imaging methane leaks have been demonstrated using infrared

Optics EXPRESS

cameras employing outdoor thermal background radiation [6]. However, the sensitivity of such systems is particularly susceptible to variations in this background temperature, which at certain times during the daily cycle may significantly reduce the sensitivity of the instrument. In an active system, the use of InGaAs laser diodes, emitting at 1.6μm, are a convenient option for the illumination source due to their compact size, allowing the development of portable systems which can detect methane in the short-wave infrared (SWIR) spectrum. However, FPAs that operate at SWIR wavelengths are less well developed than their visible wavelength equivalents, having a much reduced resolution and increased cost.

As an alternative to using a FPA it is possible to use a single photodetector and an infrared laser, wavelength tuned to an absorption line of the gas, which is raster scanned over a scene and the resulting backscattered light collected and measured [7, 8]. Infrared laser light suitable for detecting methane can be provided by many different sources including, compact distributed feedback InGaAs laser diodes operating at wavelengths around 1.6μm [7, 9, 10], optical parametric oscillators operating at wavelengths around 3.4μm [8] or carbon dioxide lasers operating around 10μm [11]. Of these sources the laser diode provides a cost effective option.

Rather than raster scanning using galvo optics, the techniques of single-pixel/computational imaging combine pattern projection and single-pixel detectors to reconstruct images [12]. One approach is to use a sequence of masks to structure the illumination light which is then projected onto the scene and to measure the resulting backscattered light using a single photodetector. The single detector, or single-pixel, is used to measure the level of correlation between a set of patterns and the scene. Knowledge of these patterns and the corresponding correlation can be computationally inverted to enable the reconstruction of the image of the scene. Here we define our masks based on Hadamard matrices [13], which are binary functions, the masks from which form a complete orthonormal set and where each pattern contains an equal number of +1's and -1's, representing 'on' and 'off' respectively for each mask. Single-pixel imaging has the benefit of being able to image at wavelengths where multi-pixel image sensors are unavailable or costly, such as in the terahertz band [14] or SWIR [15]. The availability and low cost of single-pixel detectors operating in the SWIR spectral region make single-pixel cameras much more promising as a gas imaging device. Here, we use a digital micromirror device (DMD) to pattern the output of an infrared diode laser, tuned to a methane absorption line at 1.651μm, which is then projected onto a scene containing various sources of methane. An amplified InGaAs photodiode is used as the single-pixel to measure the laser light backscattered from the scene, some of which passes through any sources of gas present.

DMDs, consisting of hundreds of thousands of individually addressable moving micromirrors, were originally developed for the display industry [16] but have also found applications in other areas including wavelength multiplexing [17], real-time infrared imaging [15, 18], multi-object spectroscopy [19] and also applied to astronomical observations [20]. They offer a method of modulating light which is fast and works over a broad range of wavelengths. DMDs can be used to implement masks representing +1 (transmitted light) and 0 (blocked), but not +1 and -1 required for a Hadamard set. To overcome this each mask is displayed as a pair of patterns where each pattern is followed by its negative allowing a differential signal to be obtained [21]. The number of mask patterns required to fully reconstruct an image frame is proportional to the linear resolution squared (this number is doubled for the differential case) and hence, limits the frame rate for high-resolution reconstructions. However, DMDs are commercially available having display rates of ~22kHz, which for relatively low-resolution applications allows near-video rate image reconstruction on a standard performance computer [18]. For the case of locating gas leaks, the resolution of the image is of secondary importance [7]. More important is the frame rate of the system which can image quickly enough to locate the source of the leak before the gas has time to diffuse away.

We demonstrate our single-pixel imaging system in the laboratory at two different reconstruc-

Optics EXPRESS

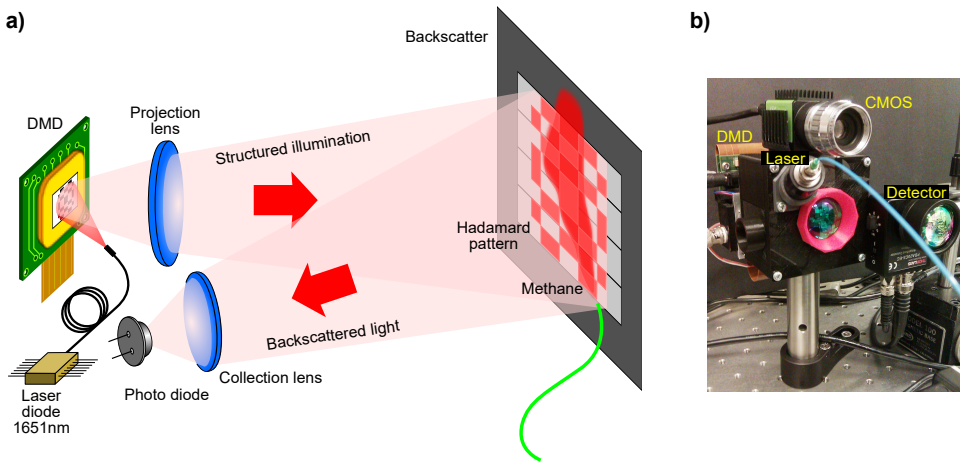

Fig. 1. Configuration of the single-pixel imaging system. a) Schematic of optical configuration. An InGaAs laser diode, operating at 1.651μm, is used to illuminate a DMD, allowing patterns displayed on the chip to be projected onto a scene using a projection lens. A lens is used to collect the total light which is backscattered from the scene, detected using a single InGaAs photodetector, and which also propagates through the methane sources. A set of orthogonal mask patterns (Hadamard matrices), and their corresponding inverse patterns, are sequentially displayed on the DMD and the backscattered intensity measured. b) Photo of optical head containing the DMD, laser fibre, CMOS camera and single-pixel detector.

tion resolutions. We image a static scene containing glass cells filled with known concentrations of methane in air, at a resolution of 64x64, which shows the individual cells and their contents. We demonstrate real-time imaging of a gas leak from a 1/4 inch diameter tube of ~0.2 litres/minute, at a resolution of 16x16 (512 masks corresponding to a full set of 16x16 pixel patterns + inverse). Although low-resolution image reconstructions are sufficient for determining the source of a gas leak, it is desirable to combine this information with high-resolution color images of the scene. For this reason, a visible camera is used to provide an image for the operator, upon which the gas data is overlaid.

2. Experimental configuration

Figure 1(a) shows an illustration of the single-pixel gas imaging camera. An infrared source consisting of a fibre coupled InGaAs laser diode (LASER 2000, LAS-022527) is used to illuminate a high-speed DMD (Vialux, V-7000). The wavelength of the laser can be coarsely tuned with temperature and finely tuned with current, both controlled using the laser driver (Thorlabs, CLD1015). The wavelength is initially set to correspond to a methane absorption transition at 1.651μm, and applying a square wave signal of ± 0.014V to the laser diode drive current modulation input allows the laser to be tuned on and off of the methane absorption allowing a differential gas measurement. The tuning rate of the laser is approximately 12 pm/mA and the 0.014V modulation corresponds to a wavelength shift of 0.05nm, larger than the absorption linewidth of methane at atmospheric pressure.

Rather than raster scanning the laser over the scene, we structure the illumination using patterns displayed on the DMD. A singlet lens, diameter 30mm and 50mm focal length, with an antireflection (AR) coating for infrared, is used to project the patterns onto the scene. The sequence of patterns is pre-loaded onto the memory buffer of the DMD and then displayed at 20kHz. The DMD chip resolution is 1024x768 with a mirror pitch = 13.7μm (DLP, Discovery

Optics EXPRESS

4100). The mirrors are binned according to the desired reconstructed resolution, using a 768 x 768 area of the chip. An AR coating on the window of the DMD chip reduces losses of the 1.65μm light. A simple low-cost, uncooled, amplified InGaAs photodiode (spectral response 800nm-1800nm) (Thorlabs, PDA20CS-EC) is used to measure the total intensity of the backscattered laser light from the scene, collected using a singlet lens, diameter 30mm and 30mm focal length, having a similar AR coating to the projection lens. Signals from the photodiode are read using a 16 bit data acquisition module (DAQ) (National Instruments, NI USB-6366), capable of sampling at 2.0MS/s. The signal capture is synchronised to the pattern update on the DMD. The same DAQ is also used to provide the square wave signal for the laser drive current modulation, enabling the laser to be tuned on and off of the methane absorption line.

The gas imaging camera is packaged as a custom 3D printed unit containing the DMD, laser fibre mount, projection lens and single-pixel backscatter detector, as shown in Fig. 1(b). The unit also includes a high-resolution color CMOS camera to provide a navigation/guide image. The gas image information is aligned and overlaid on the images from the color CMOS camera (JAI GO-5000C-USB). Custom LabVIEW (National Instruments) interface software controls the DMD, collects all single-pixel intensity measurements from the DAQ, reconstructs the gas image and overlays an upsampled smoothed gas image on the color image of the scene obtained from the CMOS camera.

3. Results

We constructed a scene consisting of four glass sample cells containing known mixtures of methane in air (0%, 25%, 50% and 100% volume), all at atmospheric pressure. The cells were all of 20mm diameter and 10mm thick and arranged in front of a background which consisted of a black cardboard screen with strips of infrared reflecting tape covering the central region. The size of the infrared reflecting region was 250mm x 200mm and the background was located 1m from the camera lens. Also included within the scene were two 1/4 inch diameter PTFE tubes used to deliver gas leaks of a predetermined flow rate (the two gases used here were pure methane and nitrogen). Needle valves with floating ball indicators allowed the flow rates through these tubes to be controlled over the range 0.1 - 5.0 litres/min. Figure 2(a) shows a photo of the gas cell arrangement in front of the reflective background. Figure 2(b) shows the methane absorption spectra at around 1.65μm, obtained from the HITRAN database [22].

The DMD memory buffer was initially loaded with 8,192 patterns, corresponding to a 4,096 Hadamard set at a resolution of 64x64 and their inverse patterns. At this resolution all four sample cells are clearly visible as shown in Fig. 2(c) and Fig. 2(d). For every alternate reconstruction frame, the wavelength of the laser was tuned either on or off the methane absorption using the laser diode current modulation input on the controller, reconstructed for a 8,192 pattern sequence. By taking the difference of the single-pixel intensity measurements between alternate frames, images can then be obtained of the gas only as shown in Fig. 2(e). The three sample cells containing methane are visible in the reconstructed difference gas image. The 64x64 resolution images are then averaged over 5 frames, smoothed and upsampled as shown in Fig. 2(f). The 5x5 kernel used to smooth the gas image is shown in the inset of Fig. 2(f).

In many imaging applications a high-resolution is the preferred option. However, in the case of single-pixel imaging there is a trade-off between the resolution and frame rate of the reconstructed images, as the number of mask patterns required is proportional to the square of the linear resolution. In addition the signal to noise ratio (SNR) scales in inverse proportion to the linear resolution for constant pattern display time [23]. Both of theses factors mean that lower resolutions are a viable and attractive option for single-pixel imaging. Figure 3 shows a single frame from the gas imaging camera. Figure 3(a) shows the low-resolution (16x16) gas image, Fig. 3(b) shows the smoothed gas image and Fig. 3(c) shows the gas image overlay. Here a total of 512 patterns are loaded onto the DMD, resulting in a reconstruction frame rate of 25 Hz. The

Optics EXPRESS

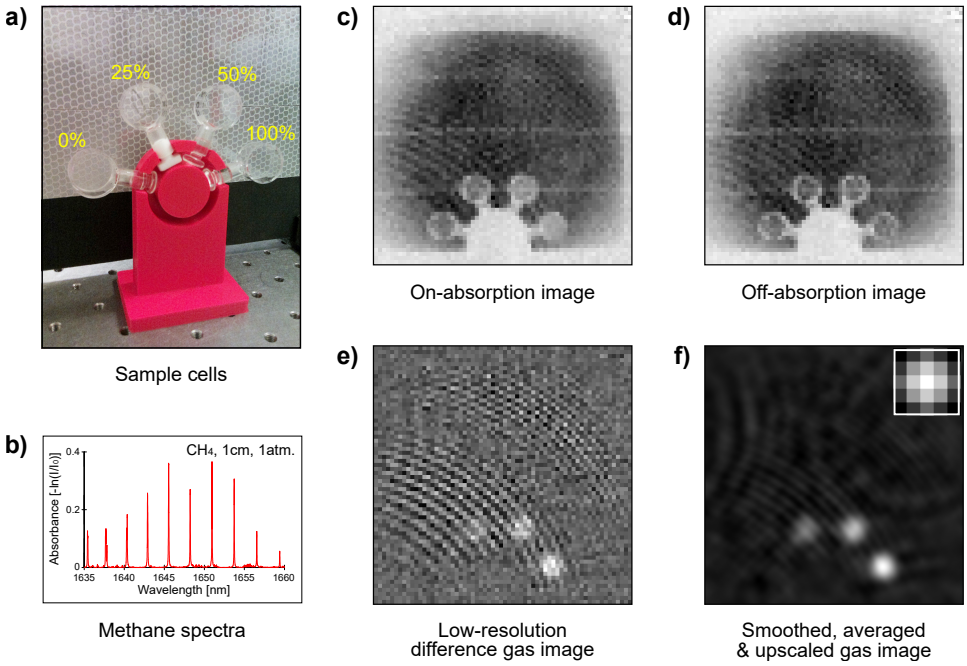

Fig. 2. a) Photo of gas sample cells located in front of the infrared reflective background. b) Methane absorption data at around 1.65μm, obtained using the HITRAN database. c-d) On and Off-absorption infrared images of gas sample cells, reconstructed at 64x64 resolution. e) Difference gas image at 64x64 resolution. f) Smoothed, averaged and upsampled gas image. Inset shows the 5x5 smoothing kernel used.

differential images are again averaged over 5 frames, and are smoothed using a 3x3 kernel as shown in inset of Fig. 3(b). Again, all of the glass cells containing methane are clearly visible which allows the gas images to be correctly scaled and aligned with high-resolution images from the color camera. To aid the operator in identifying the gas sources the upsampled images are thresholded and color coded red before being overlaid on the color image, as shown in Fig. 3(c). The CMOS camera covers a slightly larger field-of-view compared to the single-pixel camera, which allows a larger area of the scene to be viewed. The green outline box overlaid on the high-resolution image in Fig. 3(c) indicates the active area over which the gas can be detected.

In addition to imaging sample cells of fixed methane concentration, we simulate a gas leak by introducing gas from a pressurised cylinder containing 100% methane, delivered to the scene via a length of 1/4 inch diameter PTFE tube. Again the images are averaged, smoothed and upsampled before being thresholded and overlaid on the high-resolution color image. To demonstrate that our imaging system is sensitive to methane only we introduce a second gas leak to the scene from a pressurised nitrogen cylinder and show that only the methane is visible in the reconstructed image. Figure 4(a) shows representative frames from a video of a gas leak for a methane flow rate of 0.2 litres/min (delivered via the green tube shown on the right hand side of the frames). The reconstruction and smoothing frame rate for a 16x16 resolution is 25Hz and allows the source of the leak to be easily identified. Nitrogen is introduced to the scene via the red tube, shown on the left hand side of the frames, and is fixed at a flow rate of 2 litres/min. Whilst the methane leak is clearly visible the nitrogen leak is completely undetected, even when both leaks are simultaneous, as we are sensitive only to the methane absorption rather than the

Optics EXPRESS

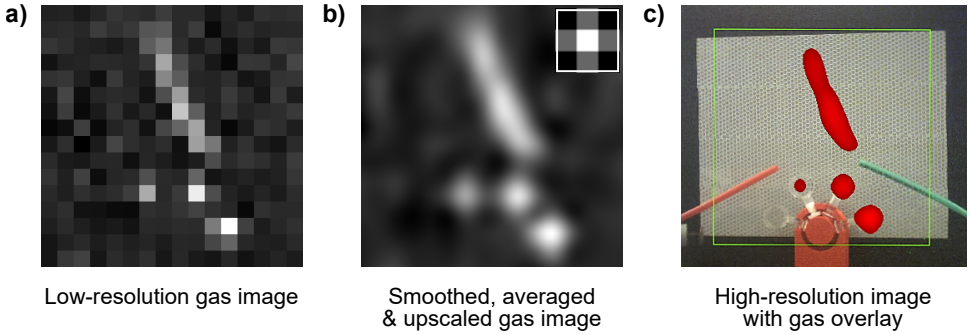

Fig. 3. a) Low-resolution (16x16) reconstructed image of gas cells and gas leak. b) Smoothed, averaged and upscaled gas image (512x512), smoothing kernel shown in figure inset. c) Color coded gas data overlaid onto a high-resolution color image from a CMOS camera.

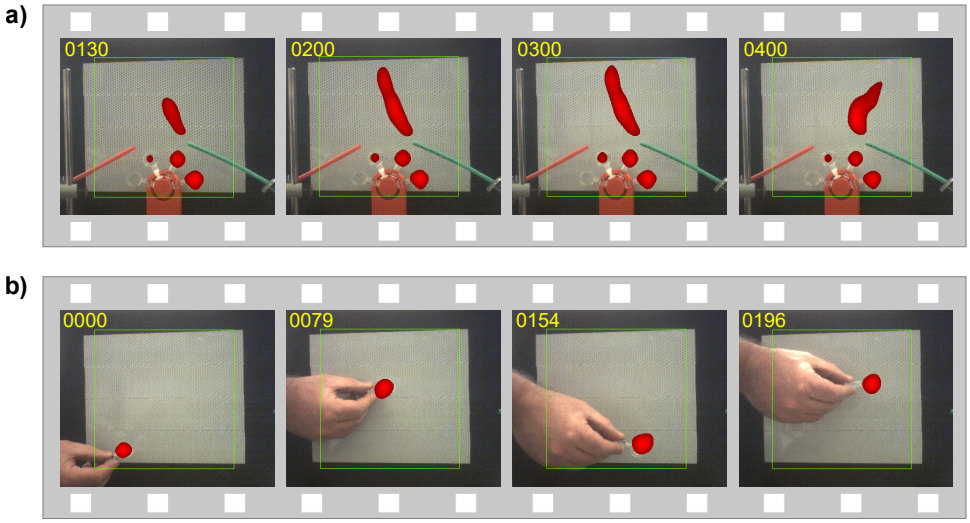

Fig. 4. a) Selected movie frames from a low-resolution (16x16) computational image of a gas leak, overlaid onto a high-resolution color image from a CMOS camera. Flow rates of 0.2 litres/min. methane and 2 litres/min. nitrogen is delivered to the scene via the green and red tubes respectively, as shown in the individual frames. Only the methane gas is detected despite the flow rate of nitrogen being large enough to perturb the methane plume, evident in frame 0400 of the movie (see (Visualization 1). b) Selected movie frames from imaging a dynamic scene where a gas sample cell is moved by hand across the field-of-view (see (Visualization 2).

Optics EXPRESS

temperature difference between the escaping gas and the background. The effect of the nitrogen leak on the methane can be seen in later frames of Fig. 4(a) where the gas plume is seen to blow towards the right. The frame rate of our system is sufficient that we are relatively insensitive to motion blur from a dynamically changing scene. As a demonstration we image a dynamic scene where one of the gas sample cells (containing 100% methane) is moved by hand across the field-of-view. Figure 4(b) shows selected frames from a recorded movie where only the gas cell is imaged despite other parts of the scene changing in real-time.

4. Discussion and conclusions

We have demonstrated that a single-pixel imaging system can be used to image gas leaks in real-time. Reducing the reconstructed resolution of the gas images to 16x16 increases the frame rate, allowing the gas to be imaged in a dynamic scene. Smoothing the 16x16 gas data still gives images of sufficient quality to allow the user to identify the source of the leak.

An alternative method for increasing the frame rate while maintaining a higher resolution is to use compressive sensing techniques, which exploit knowledge of the basis in which an image can be sparsely represented [12, 24]. A reduction in the numbers of mask patterns can also be achieved using adaptive sampling, where pattern choice is based upon previous measurements. Examples of this include guiding pattern choice using the wavelet transform [25], by motion detection [23] or in an evolutionary scheme by biasing a reduced pattern set towards those patterns that are predicted to be important based on recent measurements [15]. Using techniques such as these, compressive sensing may provide a means of imaging gas in applications where higher resolution is important.

A limitation of single-pixel imaging is the reduction in the SNR of the reconstructed images as the resolution is increased. Microscanning sets of lower resolution patterns enables an improvement in SNR with only a moderate sacrifice in reconstructed resolution. This provides a way to optimize the trade-off between SNR and resolution to suit the conditions of the scene [26].

Various research groups have investigated methods to enhance the performance of FPAs for infrared imaging. Dhar et al. [27] provides a useful review of recent advances in infrared detector technology, including the reduction of dark current noise in mid-wave infrared (MWIR) detector arrays through appropriate fabrication processes and device design. Allen et al. [28] proposes a method to increase the sensitivity and angle-of-view of MWIR detector arrays by integration with dielectric microspheres. It is anticipated that similar future advances in SWIR FPA technology will also benefit SWIR single-pixel detectors, thus improving the performance of our gas imaging system while maintaining a low-cost. A SWIR detector having an increased sensitivity and angle-of-view, in addition to a higher power laser for the illumination, should allow imaging of gas over longer distances, over larger areas and with an uncooperative backscatter. In addition, the use of a widely tunable infrared laser source will allow the imaging of various different gases thus extending the range of possible applications.

The data used to produce the content of this manuscript is available at: http://dx.doi.org/10.5525/gla.researchdata.375

Funding

This work was supported by the UK Quantum Technology Hub in Quantum Enhanced Imaging (Grant No. EP/M01326X/1) and the European Research Council (TWISTS, Grant No. 192382). DBP acknowledges support from the Royal Academy of Engineering.